ACES Asian Chemical Editorial Society

doi.org/10.1002/asia.202300266

CHEMISTRY AN ASIAN JOURNAL Research Article

www.chemasianj.org

Ferrocene-Based N-Heterocyclic Plumbylenes [Fe{(η^5-C_5H_4)$NSiMe_2R$}$_2$Pb:]: Influence of the Steric Demand of the *N*-Substituents on Their Dimerization via C–H Activation with Pb^{II}

Robin Guthardt,[a] Hannes L. Jacob,[a] Dominic Herle,[a] Michael Leibold,[a] Clemens Bruhn,[a] Myron Heinz,[b] Max C. Holthausen,[b] and Ulrich Siemeling*[a]

Dedicated to Prof. Dr. Wolfgang Weigand on the Occasion of his 65th Birthday

Abstract: Ferrocene-based N-heterocyclic plumbylenes fc[$(NSiMe_2R)_2$Pb:] (**1**; fc = 1,1′-ferrocenylene) are easily accessible by transamination from $[(Me_3Si)_2N]_2$Pb and the corresponding 1,1′-diaminoferrocene derivatives $fc(NHSiMe_2R)_2$. They may form unconventional dimers **2** by a process, which causes the cleavage of a cyclopentadienyl C–H bond and the formation of a Pb–C and an N–H bond. The monomer-dimer equilibrium (2 **1**⇆**2**) has been addressed experimentally and computationally. It critically depends on the steric demand of the *N*-substituents $SiMe_2R$, which has been varied systematically by using homologues with aliphatic (R = methyl, ethyl, isopropyl, *tert*-butyl) and aromatic units (R = phenyl, mesityl, ferrocenyl). Even in the sterically least congested case (R = methyl), dimerization is only slightly exergonic. It eventually becomes prohibitively endergonic with increasingly larger substituents and is thus not observed for R = *tert*-butyl, mesityl, and ferrocenyl. R = phenyl represents a borderline case, where the dimer is still detectable in the equilibrium mixture, albeit as a very minor component, in accord with the slightly endergonic Gibbs free energy change calculated for its formation. Addition of 4-dimethylaminopyridine (DMAP) to the monomer-dimer equilibrium mixtures cleanly affords the corresponding adducts [**1**(DMAP)], irrespective of the equilibrium composition.

Introduction

1,1′-Ferrocenylene-bridged N-heterocyclic carbenes (NHCs) of the type $fc[(NR)_2C:]$ (fc = 1,1′-ferrocenylene; Figure 1, left) were introduced in 2008 by Bielawski, who showed that the ferrocene-based backbone of these NHCs allows redox-switching of their electronic ligand properties,[1] thus opening the door to redox-tunable metal complex catalysis.[2]

The *N*-substituents chosen by Bielawski resulted in NHCs too unstable for isolation, which prohibited a study of the free carbenes. Using bulkier *N*-substituents, we have been able to obtain thermally stable congeners,[3] which turned out to exhibit a pronounced ambiphilicity similar to that of cyclic (alkyl)(amino)carbenes (CAACs), thus allowing the activation of fundamentally important small molecules like ammonia and carbon monoxide.[3c,4,5] This reactivity was unprecedented for NHCs and may be ascribed to the large $C_{carbene}$ bond angle due to the six-membered ring structure indicated in Figure 1.[3,4] This prompted us to extend our study to the heavier carbene analogues $fc[(NR)_2E:]$ (E = Si–Pb; Figure 1, right),[6] because we anticipated unconventional reactivities for such ferrocene-based N-heterocyclic tetrylenes, too. A particularly remarkable finding was made in lead chemistry, where we observed the first example of a C–H activation with Pb^{II} (Scheme 1).[6f]

The N-heterocyclic plumbylene $fc[(NSiMe_3)_2Pb:]$ (**1Me**) was found to be in equilibrium with an unprecedented type of dimer (**2Me**) in solution. The temperature dependence of this equilibrium (K = 2.8, 2.5, and 2.1 mol^{-1} L at T = 26, 30, and 34 °C, respectively, for 2 **1Me**⇆**2Me**) is in accord with the expectation that dimer dissociation is entropically favourable. According to a mechanistic DFT assessment, the initially formed conventional aggregation dimer $(\mathbf{1Me})_2$ undergoes an intramolecular electrophilic substitution by an endo attack of a Pb^{II} atom, causing the cleavage of a C–H bond and the formation of a Pb–C and an

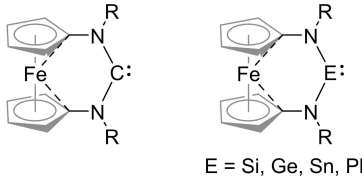

Figure 1. 1,1′-Ferrocenylene-bridged N-heterocyclic carbenes (left) and their heavier analogues (right). The structures are drawn in a way that highlights the six-membered ring structure formally present in these [3]ferrocenophane-type compounds.

[a] *R. Guthardt, H. L. Jacob, D. Herle, Dr. M. Leibold, Dr. C. Bruhn, Prof. Dr. U. Siemeling*
Institute of Chemistry
University of Kassel
Heinrich-Plett-Str. 40, 34132 Kassel (Germany)
E-mail: siemeling@uni-kassel.de

[b] *M. Heinz, Prof. M. C. Holthausen*
Institut für Anorganische und Analytische Chemie
Goethe-Universität
Max-von-Laue-Straße 7, 60438 Frankfurt am Main (Germany)
E-mail: max.holthausen@chemie.uni-frankfurt.de

Supporting information for this article is available on the WWW under https://doi.org/10.1002/asia.202300266

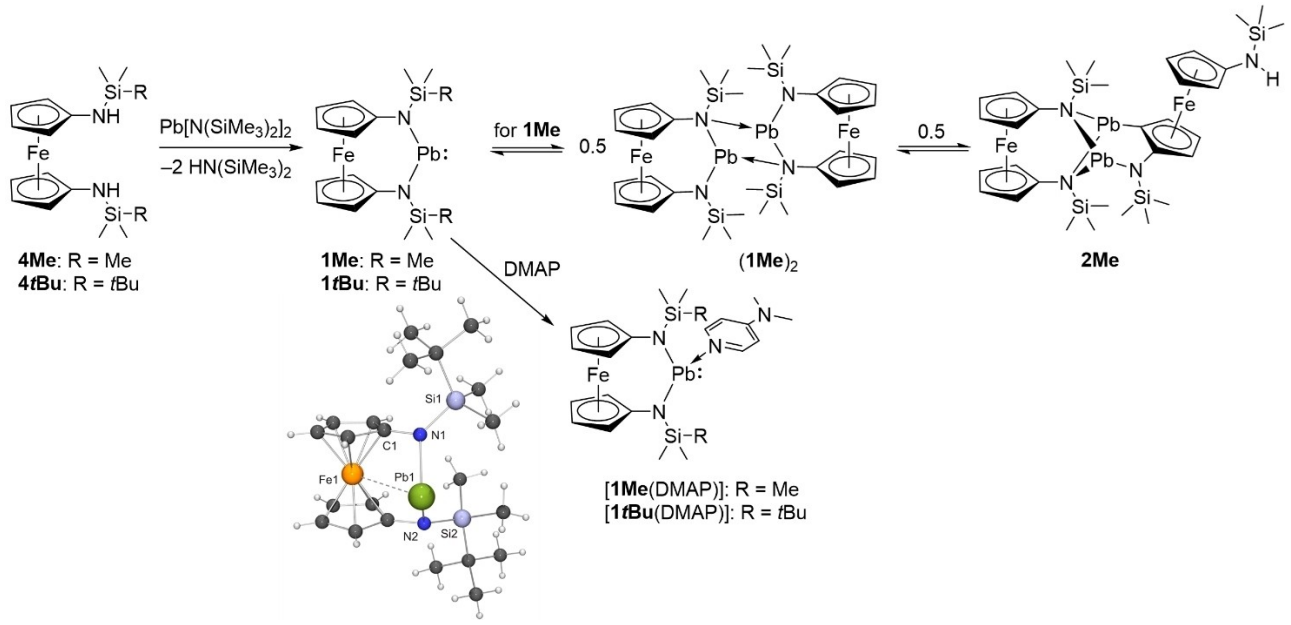

Scheme 1. Synthesis of **1Me** and **1*t*Bu** and molecular structure of **1*t*Bu** as determined by single-crystal X-ray diffraction (XRD). The "reactive" dimerization of **1Me** to **2Me** via aggregation dimer $(\mathbf{1Me})_2$ (identified computationally) and the trapping of **1Me** with 4-dimethylaminopyridine (DMAP) are also shown.

N–H bond. While crystallisation exclusively furnished dimer **2Me** (97% yield), efficient trapping of monomer **1Me** in solution was achieved with suitable Lewis bases; for example, the 4-dimethylaminopyridine (DMAP) adduct [**1Me**(DMAP)] was isolated in 99% yield by using 1 equiv. of DMAP in toluene (Scheme 1), whereas the weaker donor THF is not able to suppress dimer formation completely even if present in huge excess, viz. as solvent, according to NMR spectroscopic analysis in THF-d_8. Dimer **2Me** is planar-chiral and has proved useful for the synthesis of planar-chiral homologues of 1,1′-diaminoferrocene.[7] In contrast to the trimethylsilyl-substituted congener **1Me**, the $SiMe_2tBu$ homologue **1*t*Bu** shows no dimerization, but apparently quenches its electrophilicity by the formation of an intramolecular Fe—Pb bond (Scheme 1), leading to a half-chair conformation of the six-membered FeC_2N_2Pb ring, which is slightly more stable (by 1.2 kcal mol^{-1}) than the isomer with a planar ring according to DFT results.[6f] The situation is inverse for **1Me**, where the planar isomer was computed to be 1.1 kcal mol^{-1} more stable than the half-chair isomer. The different behaviour of **1Me** and **1*t*Bu** is plausibly ascribed to steric effects. In order to test this hypothesis, we have systematically complemented our study of **1Me** and **1*t*Bu** using the homologous series of N-heterocyclic plumbylenes fc[$(NSiMe_2R)_2$Pb:] with R = ethyl (**1Et**), isopropyl (**1*i*Pr**), phenyl (**1Ph**), mesityl (**1Mes**), and ferrocenyl (**1Fc**). We here describe the results of this investigation.

Results and Discussion

The new plumbylenes **1Et**, **1*i*Pr**, **1Ph**, **1Mes**, and **1Fc** were synthesised in analogy to **1Me** and **1*t*Bu** by transamination from the acyclic diaminoplumbylene $[(Me_3Si)_2N]_2$Pb (**3**) and the corresponding 1,1′-diaminoferrocene derivative fc$(NHSiMe_2R)_2$ (**4Et**, **4*i*Pr**, **4Ph**, **4Mes**, and **4Fc**)[8] in toluene (Scheme 2).

Ambient temperature was sufficient in the case of R = Et. The reactions of the bulkier homologues were too sluggish under these conditions so that elevated temperatures (ca. 70 °C) were used. When performed on a small scale in a sealed NMR tube, NMR spectroscopic monitoring of the reactions confirmed essentially quantitative transamination. When performed on a preparative scale, work-up therefore simply consisted of removing volatile components under reduced pressure. Crude products thus obtained were subsequently subjected to NMR spectroscopic analysis in C_6D_6, which revealed a monomer-dimer equilibrium analogous to that previously observed for **1Me**⇆**2Me**, except in the case of **1Mes** and **1Fc**, where no dimerization could be detected. **1Fc** was structurally characterised by XRD (vide infra). Our previous in-depth NMR spectroscopic study of the **1Me**⇆**2Me** equilibrium mixture in C_6D_6 had shown that the ^{207}Pb NMR spectrum exhibits three signals. The low-field signal at $\delta(^{207}Pb) = 4333$ ppm is due to the dicoordinate Pb^{II} atom of monomer **1Me**. Dimer **2Me** contains two different, and tricoordinate, Pb^{II} atoms, giving rise to two signals at higher field (3764 ppm for the Pb atom bonded to three N atoms and 2853 ppm for the Pb atom bonded to one C atom and two N atoms; see Table 1). An additional diagnostic feature of dimer **2Me** is the conspicuous low-field signal due to the plumbylated C atom at $\delta(^{13}C) = 184$ ppm.[9] The characteristic NMR spectroscopic signature of a monomer-dimer equilibrium is clearly evident for **1Et**, **1*i*Pr**, and **1Ph** from the NMR data collected in Table 1. The presence of monomer and dimer in solution leads to rather complicated ^{1}H and ^{13}C NMR spectra in those cases, where the concentrations of monomer and dimer are similar. Not surprisingly, the **1**⇆**2** equilibrium is increasingly shifted in favour of the monomer with increasing steric bulk of

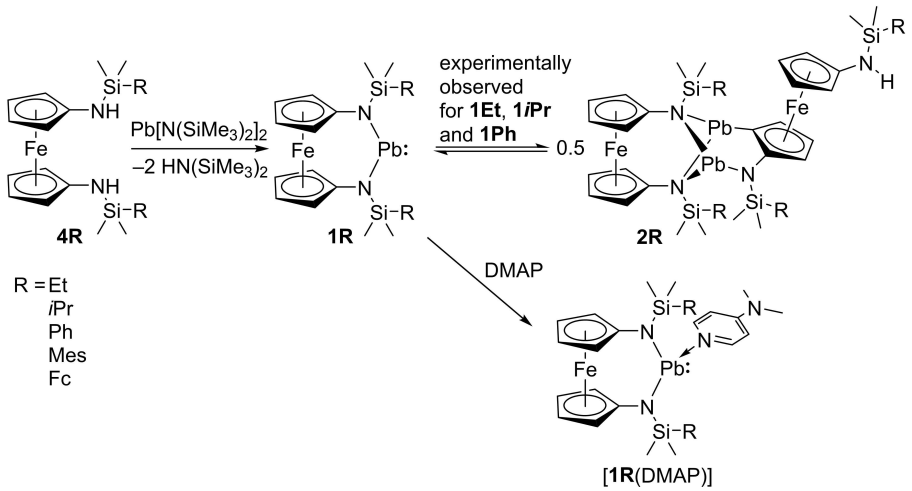

Scheme 2. Synthesis of plumbylenes **1Et**, **1*i*Pr**, **1Ph**, **1Mes**, and **1Fc** and their DMAP adducts (Mes = mesityl, Fc = ferrocenyl). **1Et**, **1*i*Pr**, and **1Ph** were found to be in equilibrium with their dimers **2Et**, **2*i*Pr**, and **2Ph** in benzene solution.

Table 1. Pertinent NMR spectroscopic data (C_6D_6) of the Pb^{II} compounds of this study.

	$\delta(^{207}Pb)$	$\delta(^{13}C)$ PbC (**2**)
1Me ⇆ **2Me**	4333;[a] 3764, 2853[b]	184
1Et ⇆ **2Et**	4260;[a] 3757, 2861[b]	184
1*i*Pr ⇆ **2*i*Pr**	3926;[a] 3494, 3098[b]	186
1*t*Bu	2550	
1Ph ⇆ **2Ph**	3821;[a] n.d.[c]	187
1Mes	4258	
1Fc	3913	
[**1Me**(DMAP)]	3017	
[**1*t*Bu**(DMAP)]	2999	
[**1Et**(DMAP)]	3010	
[**1*i*Pr**(DMAP)]	3023	
[**1Ph**(DMAP)]	2928	
[**1Mes**(DMAP)]	3121	
[**1Fc**(DMAP)]	2991	

[a] Signal of monomeric plumbylene **1**. [b] Signals of plumbylene dimer **2**. [c] Signals due to **2Ph** could not be detected.

R. In the case of R = *i*Pr the dominance of the monomeric plumbylene in the mixture already allowed unequivocal signal assignments for **1*i*Pr**. With R = Ph only the monomeric plumbylene **1Ph** was detectable by ^{207}Pb NMR spectroscopy in concentrated C_6D_6 solution. However, closer inspection of the ^1H, ^{13}C, and ^{29}Si NMR spectra (see Figures S22–S24 in the Supporting Information) revealed the presence of dimer **2Ph** as a very minor component. This behaviour is in line with the corresponding Winstein–Holness *A*-value,[10] which is an established measure of the steric size of a substituent, increasing in the order Me (1.7) < Et (1.8) < *i*Pr (2.2) < Ph (2.8).[11]

The ^1H and ^{13}C NMR spectra of the monomeric plumbylenes **1** are indicative of a C_{2v} symmetric structure on the NMR time scale. The 1,1′-ferrocenylene protons give rise to the highly symmetric pattern expected for an AA′BB′ spin system (observed in the spectral region between ca. 3.9 and 3.5 ppm as two signals integrating for 4 protons each). The trimethylsilyl substituents of **1Me** (R = Me) give rise to a singlet at $\delta(^1H)$ = 0.16 ppm integrating for 18 protons. In the other cases (R ≠ Me), a single signal is observed for the 12 $SiMe_2$ protons, located in the spectral region between ca. 0.5 and 0.1 ppm. Signal assignments are straightforward in those cases, where the monomeric plumbylene is predominantly (R = *i*Pr, Ph) or exclusively present (R = Mes, Fc, *t*Bu). The *t*Bu groups of **1*t*Bu** are observed as a singlet integrating for 18 protons at $\delta(^1H)$ = 1.01 ppm. The *i*Pr groups of **1*i*Pr** give rise to a doublet at $\delta(^1H)$ = 1.01 ppm integrating for 12 protons. The corresponding C*H*Me_2 signal is probably located at $\delta(^1H)$ = 0.85 ppm (br., 4H), but could not be identified with certainty due to the presence of several broadened signals of similar integrals in the spectral region around 1.0 ppm. The Ph groups of **1Ph** cause two multiplets at $\delta(^1H)$ = 7.64 and 7.19 ppm, integrating for 4 and 6 protons, respectively. The Mes substituents present in **1Mes** give rise to two singlets at $\delta(^1H)$ = 2.49 and 2.11 ppm, integrating for 12 and 6 protons for the *o*-Me and *p*-Me groups, respectively; in addition, a singlet at $\delta(^1H)$ = 6.63 ppm is observed for the 4 aromatic protons. The C_5H_5 protons of the ferrocenyl substituents of **1Fc** are observed as a singlet at $\delta(^1H)$ = 4.00 ppm and the ferrocenyl C_5H_4 protons give rise to two signals integrating for 4 protons each, located at $\delta(^1H)$ = 4.19 and 4.08 ppm. The 1,1′-ferrocenylene backbone of these monomeric plumbylenes causes three ^{13}C NMR signals, viz. a low-field signal with a chemical of ca. 108 ppm for the C_{ipso} atoms and two signals at $\delta(^{13}C) \approx 70$ and 75 ppm for the CH units. The $SiMe_2$ units are observed as a high-field ^{13}C NMR signal in the spectral region between ca. 8 (R = Mes) and −2 ppm (R = *t*Bu). The two R substituents present in these monomeric plumbylenes give rise to a single set of ^{13}C NMR signals in each case. Two signals at $\delta(^{13}C)$ = 27.5 and 20.8 ppm are observed for the *t*Bu substituent of **1*t*Bu**. The *i*Pr substituents of **1*i*Pr** also give rise to two signals, which are located at $\delta(^{13}C)$ = 18.2 and 16.3 ppm. Four signals are observed for the Ph substituents of **1Ph**, which are located in the aromatic region between ca. 142 and 128 ppm. The Mes substituents of **1Mes** also give rise to four signals in the aromatic region between ca. 145 and 130 ppm; in addition, two

signals are observed at $\delta(^{13}C) = 25.5$ and 21.2 ppm for the *o*-Me and *p*-Me groups, respectively. The ferrocenyl moieties of **1Fc** cause an intense signal due to the C_5H_5 rings at $\delta(^{13}C) =$ 68.8 ppm and three signals for the C_5H_4 unit located at $\delta(^{13}C) =$ 74.1, 71.7, and 71.4 ppm (C_{ipso}).

The DMAP adducts of **1Me**–**1Fc** were obtained in excellent yields upon addition of DMAP (1 equiv.) to the respective transamination reaction mixture in toluene (Scheme 2). Structural characterisation by XRD was possible in each case, proving the tricoordinate nature of the divalent lead atom (vide infra). The $\delta(^{207}Pb)$ values of the DMAP adducts of **1Me**–**1Fc** lie in the narrow range from 2991 to 3121 ppm (Table 1), in accord with tricoordinate Pb^{II}.[12] The signals due to the respective plumbylene unit in the ^1H and ^{13}C NMR spectra of these adducts are compatible with a time-averaged C_{2v} symmetric structure in each case. A comparison of the ^1H and ^{13}C NMR spectra of the plumbylenes **1*t*Bu**, **1Mes**, and **1Fc**, whose behaviour is particularly simple (no dimerization), with those of their DMAP adducts reveals that DMAP coordination does not cause a change in the number of the signals due to the respective plumbylene. However, significant DMAP-induced chemical shift changes can be made out. For example, a downfield shift of ca. 6–10 ppm is observed for the ^{13}C NMR signal due to the respective fc C_{ipso} atoms. This behaviour indicates that the dissociation-association equilibrium [**1**(DMAP)] $\leftrightarrows$ **1** + DMAP is fast on the NMR time scale. This situation is similar to that encountered before for adducts of **1Me** and **1*t*Bu** with the N-heterocyclic olefin 1,3,4,5-tetramethyl-2-methyleneimidazoline.[6c] Note that the high-field shifted signal observed at $\delta(^{207}Pb) = 2550$ ppm for plumbylene **1*t*Bu** is in line with the tricoordinate nature of its Pb^{II} atom due to the intramolecular Fe–Pb bond identified by XRD and DFT (Scheme 1).[6f] In contrast, the new plumbylenes **1Ph**, **1Mes**, and **1Fc** exhibit ^{207}Pb NMR signals typical of dicoordinate Pb^{II},[13] which was in fact confirmed by XRD for **1Fc** (Figure 2). **1Ph** and **1Mes** were obtained as oils which unfortunately resisted crystallisation.

Pertinent metric parameters of the structurally characterised Pb^{II} compounds are collected in Table 2. The molecular structures of the DMAP adducts of **1*i*Pr**, **1Mes**, and **1Fc** are exemplarily shown in Figures 3–5 (see the Supporting Information for the other new DMAP adducts of this study).

The Fe–Pb distances lie in the small range between ca. 4.00 Å (for [**1*t*Bu**(DMAP)]) and 4.11 Å (for [**1Fc**(DMAP)]). The notable exception is plumbylene **1*t*Bu**, whose Fe–Pb distance of only 3.265(2) Å reflects the presence of an intermetallic bond.[6f] **1*t*Bu** exhibits a large fold angle φ of 71.6°, corresponding to a half-chair conformation of the six-membered FeC_2N_2Pb ring. In contrast, plumbylene **1Fc** contains no such bond and exhibits an essentially planar FeC_2N_2Pb ring with negligible folding (φ 1.3°). The Pb–N_{amino} bond lengths of **1Fc** are slightly shorter than the corresponding bond lengths of its adduct

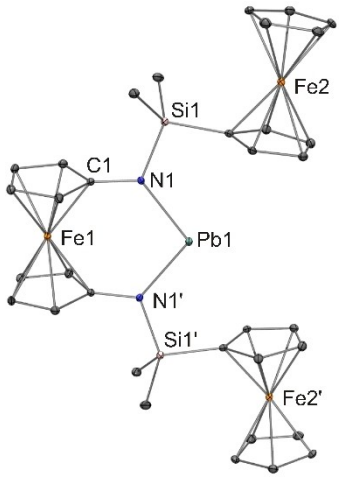

Figure 2. Molecular structure of **1Fc**·C_6H_6 in the crystal (ORTEP with 30% probability ellipsoids; hydrogen atoms and solvent molecule omitted for clarity).

Table 2. Pertinent metric parameters of **1*t*Bu** and **1Fc** and of the DMAP adducts of **1Me**–**1Fc**.

	Pb–N_{amino}	Pb–N_{DMAP}	N_{amino}–Pb–N_{amino}	Fold angle φ[a]	Coordination angle ϱ[b]	DMAP tilt angle τ[c] $\Sigma\angle N_{DMAP}$
1*t*Bu[d]	2.240(10)		99.2(4)	71.6		
	2.291(12)					
1Fc·C_6H_6	2.184(3)		100.21(14)	1.3		
[**1Me**(DMAP)]·$^1/_2C_6H_6$[d]	2.211(3)	2.496(3)	99.89(12)	20.0	91.1	15.1
	2.205(3)					357.7
[**1*t*Bu**(DMAP]	2.224(2)	2.497(2)	97.67(8)	31.2	97.6	18.5
	2.230(2)					357.0
[**1Et**(DMAP)]	2.221(6)	2.500(7)	99.7(2)	20.3	91.7	14.7
	2.206(6)					357.8
[**1*i*Pr**(DMAP)]	2.223(2)	2.494(2)	98.32(6)	25.2	94.2	18.6
	2.210(2)					356.5
[**1Ph**(DMAP)]	2.236(3)	2.437(3)	99.46(11)	24.7	94.9	4.3
	2.239(3)					359.6
[**1Mes**(DMAP)]	2.231(7)	2.417(8)	98.1(3)	24.6	95.4	21.4
	2.244(9)					355.2
[**1Fc**(DMAP)]	2.227(4)	2.499(7)	98.2(2)	8.9	91.1	1.5
						359.9

[a] Dihedral angle between the best plane of the two cyclopentadienyl C_{ipso} and their adjacent N_{amino} atoms and the PbN_2 plane formed by the Pb and the two N_{amino} atoms. [b] N_{DMAP}–Pb–(PbN_2 centroid) angle. [c] Pb–N_{DMAP}–(DMAP centroid) angle. [d] Ref. [6f].

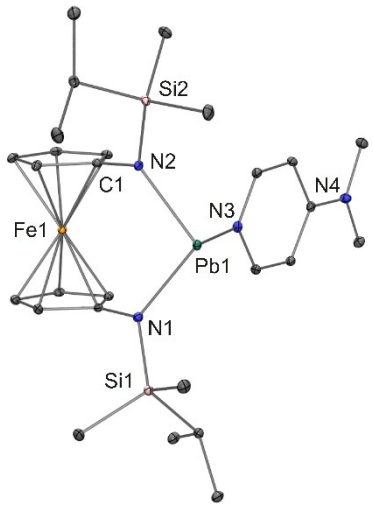

Figure 3. Molecular structure of [1*i*Pr(DMAP] in the crystal (ORTEP with 30% probability ellipsoid; hydrogen atoms omitted for clarity).

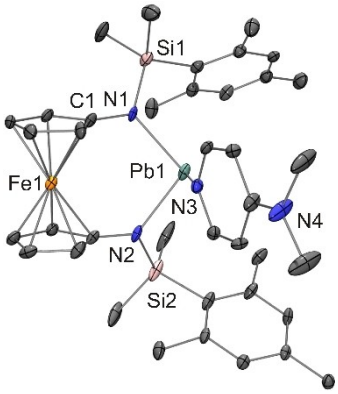

Figure 4. Molecular structure of [**1Mes**(DMAP] in the crystal (ORTEP with 30% probability ellipsoids; hydrogen atoms omitted for clarity).

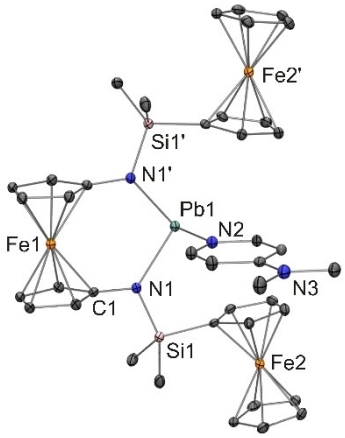

Figure 5. Molecular structure of [**1Fc**(DMAP] in the crystal (ORTEP with 30% probability ellipsoids; hydrogen atoms omitted for clarity).

[**1Fc**(DMAP)] (2.18 vs. 2.23 Å), thus reflecting the dicoordinate vs. tricoordinate nature of the respective Pb^{II} atom. As expected for a coordinative bond, the Pb–N_{DMAP} bond of [**1Fc**(DMAP)] is substantially longer (2.50 Å). The Pb–N distances of [**1Fc**(DMAP)] are indistinguishable within experimental error from the corresponding distances of [**1*t*Bu**(DMAP)]. The Pb^{II} atom of **1*t*Bu** is tricoordinate due to the Fe–Pb bond and its Pb–N_{amino} bonds are even slightly longer than the corresponding bonds of its adduct [**1*t*Bu**(DMAP)] (2.27 vs. 2.23 Å on average). With coordination angles ϱ between 91.1° and 97.6°, the Pb–N_{DMAP} bond vector is almost perpendicular to the plumbylene PbN_2 plane in each case, indicating that the donor-acceptor interaction involves the vacant Pb^{II} p-orbital. The data collected in Table 2 reveal no substantial differences among the DMAP adducts, except for the fact that the Pb–N_{DMAP} bonds of [**1Ph**(DMAP)] and [**1Mes**(DMAP)] are significantly shorter in comparison to the other five adducts (average values: 2.43 vs. 2.50 Å). This probably reflects a higher electrophilicity and Lewis acidity of the Pb^{II} atoms of **1Ph** and **1Mes** due the presence of the aryl groups as opposed to the more strongly σ-donating ferrocenyl or alkyl groups present in the other compounds. The orientation of the DMAP ring with respect to the cyclopentadienyl rings of the fc backbone is approximately perpendicular in all cases except [**1Fc**(DMAP)], where an essentially parallel alignment is observed (Figure 5). An additional peculiar feature of [**1Fc**(DMAP)] is the fact that its N_{DMAP} atom is trigonal planar (sum of angles 359.9°). This is also observed for [**1Ph**(DMAP)] (sum of angles 359.6°), whereas noticeable pyramidalisation occurs in the other cases, which, although not pronounced (sum of angles 355.2°–357.8°), results in substantial deviations of the Pb–N_{DMAP} bond vector from the DMAP ring plane, as is reflected by tilt angles τ between ca. 15° and 21°. A similar tilt angle (τ 15°) is also observed for the DMAP adduct of $[(Me_3Si)_2N]_2Pb$,[6f] but not for [{*o*-$C_6H_4(NSiMe_3)_2Pb$}(DMAP)] (τ 3°)[6f] and [{(2,6-$Me_2C_6H_3S)_2Pb$}(DMAP)] (τ 4°),[14] which are the only other structurally characterised plumbylene-DMAP adducts containing tricoordinate Pb^{II} known to date. The reasons for these substantial tilt angle differences are as yet unclear and we refrain from speculation in this context.

To further elucidate the different behaviour of plumbylenes **1Ph**, **1Mes**, and **1Fc**, whose $SiMe_2R$ units contain aromatic groups (R = Ph, Mes, Fc), we performed quantum-chemical calculations on the full molecular systems. We compute the dimerization slightly endergonic for the Ph homologue **1Ph** ($\Delta G = 0.9$ kcal mol^{-1}) and it becomes more endergonic for the Fc and Mes homologues ($\Delta G = 3.1$ and 6.7 kcal mol^{-1}, respectively), in line with the experimental detection of only very small amounts of dimer **2Ph** and the absence of any indication for dimer formation for R = Fc and Mes. For all three compounds the energetically lowest conformer features local C_s symmetry, with the Pb atom bent out of the Fe–N–N plane. In all three structures, however, the computed Fe–Pb distance is significantly longer than in the *t*Bu homologue **1*t*Bu** (3.27 Å for R = *t*Bu vs. 3.56, 3.78, and 3.71 Å for R = Ph, Mes, and Fc, respectively).[6f] Correspondingly, detailed analysis by means of Bader's quantum theory of atoms in molecules (QTAIM) reveals the absence of Fe–Pb bond paths for **1Ph**, **1Mes**, and **1Fc**. We identified instead multiple bond paths between Pb and the aromatic substituents, and among the latter. The respective bond critical point properties indicate closed-shell interactions

closely resembling those computed for parallel and t-stacked benzene dimers. With individual interactions between the aromatic substituents of the order of 2 kcal mol^{-1} (see the Supporting Information for benzene dimer results) it therefore seems likely that the specific structures result from an interplay of attractive intramolecular interactions within the substituent framework. In the solid state, however, additional intermolecular interactions increase complexity so that we abstain from a more detailed analysis.

Conclusion

Depending on the steric demand of their *N*-substituents, ferrocene-based N-heterocyclic plumbylenes fc[(NSiMe$_2$R)$_2$Pb:] (**1**) can form unconventional dimers **2** by a process which may be described as an electrophilic aromatic substitution and involves the cleavage of a C–H bond and the formation of a Pb–C and an N–H bond. Even in the case of SiMe$_3$ (R = Me), which is the least bulky *N*-substituent studied, dimerization (2 **1Me**→**2Me**) is only slightly exergonic at ambient temperature ($\Delta G_R = -0.6$ kcal mol^{-1}) according to ^{1}H NMR spectroscopic analysis.[6f] Dimerization eventually becomes endergonic with increasingly larger substituents. This is the case for R = Ph, where dimer **2Ph** was detected as a very minor component only in the equilibrium mixture by NMR spectroscopy. In accord with this, a slightly endergonic Gibbs free energy change of $\Delta G = 0.9$ kcal mol^{-1} was calculated for the formation of **2Ph** by dimerization of **1Ph**. Dimerization becomes prohibitively endergonic for R = Mes and Fc, which are aromatic groups larger than Ph. Consequently, only the monomeric plumbylene (**1Mes**, **1Fc**) could be detected in these cases, whose behaviour is essentially identical to that of **1*t*Bu** containing the bulky *t*Bu group.[6f]

Experimental Section

All reactions involving air-sensitive compounds were performed in an inert atmosphere (argon or dinitrogen) by using standard Schlenk techniques or a conventional glovebox. Starting materials were procured from standard commercial sources and used as received. The synthesis of **1Me** (formed in equilibrium with **2Me**) and the preparation of **1*t*Bu**, **2Me**, [**1Me**(DMAP)], and [**1*t*Bu**(DMAP)] have already been described by us in a previous publication.[6f] [(Me$_3$Si)$_2$N]$_2$Pb,[15] fc(NH$_3$)$_2$Cl$_2$,[16] SiClMe$_2$Mes,[17] SiClMe$_2$Fc,[18] and fc(NHSiMe$_2$Ph)$_2$ (**4Ph**)[19] were synthesised by adapted versions of the published procedures. NMR spectra were recorded at ambient temperature with Varian NMRS-500 and MR-400 spectrometers operating at 500 and 400 MHz, respectively, for ^{1}H. Elemental analyses were carried out with a HEKAtech Euro EA-CHNS elemental analyser at the Institute of Chemistry, University of Kassel, Germany.

Synthesis of 4Et: Dichloromethane (40 mL) was added to fc(NH$_3$)$_2$Cl$_2$ (1.04 g, 3.6 mmol) and SiClMe$_2$Et (1.23 g, 10.0 mmol). The suspension was frozen by immersion in a liquid nitrogen bath. NEt$_3$ (1.81 g, 17.9 mmol) was added. The mixture was allowed to warm up to room temperature with stirring. After 15 h volatile components were removed under reduced pressure. *n*-Hexane (10 mL) was added to the residue. Insoluble material was removed by filtration through a Celite pad, which was subsequently extracted with *n*-hexane (3×5 mL). The filtrate and extracts were combined. Volatile components were removed under reduced pressure. This afforded the product as an orange oil. Yield 1.16 g (83%). ^{1}H NMR (C_6D_6): $\delta = 3.83$, 3.79 (2 s, 2×4 H, fc), 2.04 (s, 2 H, NH), 0.96 ("t", apparent $J_{HH} = 7.8$ Hz, 6 H, CH$_2$C*H*$_3$), 0.63 ("q", apparent $J_{HH} = 8.3$ Hz, 4 H, C*H*$_2$CH$_3$), 0.14 ppm (s, 12 H, SiMe$_2$). ^{13}C{^{1}H} NMR (C_6D_6): $\delta = 105.9$ (CN), 64.6, 60.6 (2×cyclopentadienyl CH), 8.7 (CH$_2$CH$_3$), 7.5 (CH$_2$), −1.8 ppm (SiMe$_2$). ^{29}Si{^{1}H} NMR (C_6D_6): $\delta = 4.2$ ppm.

Synthesis of 4*i*Pr: This compound was obtained as a viscous orange oil by a procedure analogous to that described for **4Et** from fc(NH$_3$)$_2$Cl$_2$ (1.20 g, 4.2 mmol), SiClMe$_2$*i*Pr (1.15 g, 8.4 mmol), and NEt$_3$ (2.53 g, 25.0 mmol). Yield 1.47 g (86%). ^{1}H NMR (C_6D_6): $\delta = 3.82$, 3.80 (2 m, 2×4 H, fc), 2.05 (s, 2 H, NH), 0.98 (d, $J_{HH} = 6.7$ Hz, 12 H, CH*Me*$_2$), 0.90 (sept, $J_{HH} = 6.7$ Hz, 2 H, C*H*Me$_2$), 0.13 ppm (s, 12 H, SiMe$_2$). ^{13}C{^{1}H} NMR (C_6D_6): $\delta = 105.7$ (CN), 64.5, 60.9 (2×cyclopentadienyl CH), 17.6 (CH*Me*$_2$), 14.7 (*C*HMe$_2$), −3.4 ppm (SiMe$_2$). ^{29}Si{^{1}H} NMR (C_6D_6): $\delta = 5.8$ ppm.

Synthesis of 4Mes: This compound was obtained by a procedure analogous to that described for **4Et** from fc(NH$_3$)$_2$Cl$_2$ (2.19 g, 7.6 mmol), SiClMe$_2$Mes (3.23 g, 15.2 mmol), and NEt$_3$ (7.29 g, 72.0 mmol). Recrystallisation from diethyl ether furnished the product as an orange crystalline solid. Yield 2.02 g (47%). $C_{32}H_{44}N_2FeSi_2$ (568.72): C 67.58, H 7.80, N 4.93%; found: C 67.50, H 7.58, N 4.70%. ^{1}H NMR (C_6D_6): $\delta = 6.73$ (s, 4 H, C$_6$*H*$_2$Me$_3$), 3.74, 3.67 (2 s, 2×4 H, fc), 2.43 (s, 12 H, *o*-Me), 2.12, (s, 6 H, *p*-Me), 2.04 (s, 2 H, NH), 0.50 ppm (SiMe$_2$). ^{13}C{^{1}H} NMR (C_6D_6): $\delta = 144.7$, 139.0, 131.8 (3×C$_{quat}$ Mes), 129.8 (CH Mes), 107.2 (CN), 64.6, 59.5 (2×cyclopentadienyl CH), 24.8 (*o*-Me), 21.1 (*p*-Me), 4.4 ppm (SiMe$_2$).

Synthesis of 4Fc: This compound was obtained by a procedure analogous to that described for **4Et** from fc(NH$_3$)$_2$Cl$_2$ (1.14 g, 3.9 mmol), SiClMe$_2$Fc (2.20 g, 7.9 mmol), and NEt$_3$ (1.92 g, 19.0 mmol). Recrystallisation from *n*-hexane furnished the product as an orange crystalline solid. Yield 1.56 g (56%). $C_{34}H_{40}N_2Fe_3Si_2$ (700.40): C 58.30, H 5.76, N 4.00%; found: C 58.58, H 5.53, N 3.92%. ^{1}H NMR (C_6D_6): $\delta = 4.22$, 4.13 (2 m, 2×4 H, C$_5$H$_4$), 3.99 (s, 10 H, C$_5$H$_5$), 3.78, 3.74 (2 m, 2×4 H, C$_5$H$_4$), 2.27 (s, 2 H, NH), 0.45 ppm (SiMe$_2$). ^{13}C{^{1}H} NMR (C_6D_6): $\delta = 105.9$ (CN), 73.8, 71.6 (2×cyclopentadienyl CH), 70.9 (C$_{ipso}$Si), 68.8 (C$_5$H$_5$), 64.2, 60.2 (2×cyclopentadienyl CH), −0.7 ppm (SiMe$_2$).

Synthesis of 1Et (in equilibrium with 2Et): A solution of **4Et** (150 mg, 0.39 mmol) and [(Me$_3$Si)$_2$N]$_2$Pb (204 mg, 0.39 mmol) in toluene (3 mL) was stirred for 24 h. Volatile components were removed under reduced pressure. The residue was subjected to NMR spectroscopic analysis in C_6D_6, which revealed that the solution contained **1Et** and **2Et** as well as small amounts of residual toluene. NMR data are given without detailed signal assignments to **1Et** or **2Et**, except in unequivocal cases. Yield 232 mg (quantitative). ^{1}H NMR (C_6D_6): $\delta = 4.33$, 4.24, 4.09, 3.97, 3.94, 3.91, 3.83, 3.79, 3.68, 3.54 (cyclopentadienyl), 2.06 (NH **2c**), 1.19–0.59 (several overlapping m, Et), 0.57, 0.51, 0.47, 0.42, 0.18, 0.15, 0.08, −0.13, −0.14 ppm (9 s, SiMe$_2$). ^{13}C{^{1}H} NMR (C_6D_6): $\delta = 184.3$ (PbC **2Et**), 129.4, 113.2, 106.2, 104.8, 104.1 (5×CN), 73.9, 72.8, 71.8, 71.0, 70.7, 70.1 (two closely spaced signals), 66.9, 66.8, 66.6, 66.5, 66.1, 65.2, 64.6, 60.1, 57.1 (16×cyclopentadienyl CH), 10.9, 10.1, 9.7, 9.6, 8.8, 8.6, 8.1 (two isochronous signals according to signal intensity), 8.0, 7.5 (10×ethyl CH$_2$ and CH$_3$), 3.4, 1.3, 0.8, 0.4, 0.1, −0.1, −0.2, −0.5, −0.9 ppm (9×SiMe$_2$). ^{29}Si{^{1}H} NMR (C_6D_6): $\delta = 14.5$, 13.6, 9.8, 3.8, 3.3 ppm. ^{207}Pb NMR (C_6D_6): $\delta = 4260$ (**1Et**), 3757, 2861 ppm (2×**2Et**).

Synthesis of 1*i*Pr (in equilibrium with 2*i*Pr): The synthesis was performed in analogy to **1Et**, furnishing a mixture of **1*i*Pr** and **2*i*Pr** in quantitative yield. Residual amounts of toluene and (Me$_3$Si)$_2$NH could not be removed despite heating to 40 °C under dynamic vacuum. NMR data for **1*i*Pr** (dominant): ^{1}H NMR (C_6D_6): $\delta = 3.83$, 3.66 (2×br., 2×4 H, fc), 1.01 (d, $J_{HH} = 7.4$ Hz, 12 H, CH*Me*$_2$), 0.13 ppm

(s, 12 H, $SiMe_2$); the $CHMe_2$ signal is mostly likely located at 0.85 ppm (br., 4 H). $^{13}C\{^1H\}$ NMR (C_6D_6): $\delta = 111.2$ (CN), 69.7, 65.4 (2× cyclopentadienyl CH), 18.2 ($CHMe_2$), 16.3 ($CHMe_2$), −1.2 ppm ($SiMe_2$). ^{207}Pb NMR (C_6D_6): $\delta = 3926$ ppm. Selected characteristic NMR data for **2*i*Pr**: $^{13}C\{^1H\}$ NMR (C_6D_6): $\delta = 186.4$ (PbC), 128.4, 106.3, 104.5, 103.7 (4×CN). ^{207}Pb NMR (C_6D_6): $\delta = 3494$, 3098 ppm.

Synthesis of 1Ph: A solution of **4Ph** (495 mg, 0.72 mmol) and $[(Me_3Si)_2N]_2Pb$ (379 mg, 0.72 mmol) in toluene (6 mL) was heated to 70 °C for 3 h. The heating bath was removed. Volatile components were removed under reduced pressure, furnishing the product as a dark reddish brown oil. Small amounts of residual toluene and $(Me_3Si)_2NH$ could not be removed completely despite heating to 40 °C under dynamic vacuum. Yield 410 mg (68%).^1H NMR (C_6D_6): $\delta = 7.64$ (m, 4 H, Ph), 7.19 (m, 6 H, Ph), 3.88, 3.84 (2 m, 2×4 H, fc), 0.44 ppm (s, 12 H, $SiMe_2$). $^{13}C\{^1H\}$ NMR (C_6D_6): $\delta = 141.0$ (Ph C_{ipso}), 134.4, 129.6, 128.4 (3×Ph CH), 109.1 (CN), 68.7, 65.6 (2×cyclopentadienyl CH), 1.4 ppm ($SiMe_2$). $^{29}Si\{^1H\}$ NMR (C_6D_6): $\delta = -1.9$ ppm (low-intensity signals at 3.5, 2.0, −1.3, and −8.0 ppm are ascribed to **2Ph**). ^{207}Pb NMR (C_6D_6): $\delta = 3821$ ppm. Selected characteristic NMR data for **2Ph**: $^{13}C\{^1H\}$ NMR (C_6D_6): $\delta = 187.4$ (PbC); prolongued data collection (3 d) was necessary to observe this signal.

Synthesis of 1Mes: A solution of **4Mes** (300 mg, 0.53 mmol) and $[(Me_3Si)_2N]_2Pb$ (280 mg, 0.53 mmol) in toluene (2 mL) was heated to 70 °C for 3 h. The heating bath was removed. Volatile components were removed under reduced pressure, furnishing the product as a dark reddish brown oil. Yield 392 mg (96%). ^1H NMR (C_6D_6): $\delta = 6.63$ (s, 4 H, $C_6H_2Me_3$), 3.89, 3.79 (2 m, 2×4 H, fc), 2.49 (s, 12 H, *o*-Me), 2.11 (s, 6 H, *p*-Me), 0.51 ppm (s, 12 H, $SiMe_2$). $^{13}C\{^1H\}$ NMR (C_6D_6): $\delta =$ 144.8, 139.1, 133.2 (3×C_{quat} Mes), 129.9 (CH Mes), 109.4 (CN), 69.8, 65.3 (2×cyclopentadienyl CH), 25.5 (*o*-Me), 21.1 (*p*-Me), 7.9 ppm ($SiMe_2$). $^{29}Si\{^1H\}$ NMR (C_6D_6): $\delta = -2.4$ ppm. ^{207}Pb NMR (C_6D_6): $\delta =$ 4258 ppm.

Synthesis of 1Fc: A solution of **4Fc** (100 mg, 0.14 mmol) and $[(Me_3Si)_2N]_2Pb$ (76 mg, 0.14 mmol) in benzene (2 mL) was heated to 70 °C for 3 h. The heating bath was removed and the mixture was subsequently cooled briefly in an ice-bath. Volatile components were removed from the cold solution under reduced pressure, furnishing the product as a dark reddish brown crystalline solid. Yield 124 mg (96%). $C_{34}H_{38}N_2Fe_3PbSi_2$ (905.60): C 45.09, H 4.23, N 3.09%; found: C 44.62, H 4.50, N 2.67%. ^1H NMR (C_6D_6): $\delta = 4.19$ 4.08 (2 m, 2×4 H, Fc C_5H_4), 4.00 (s, 10 H, C_5H_5), 3.88, 3.74 (2 m, 2×4 H, fc C_5H_4), 0.45 ppm (s, 12 H, $SiMe_2$). $^{13}C\{^1H\}$ NMR (C_6D_6): $\delta = 108.8$ (CN), 74.1, 71.7 (2×cyclopentadienyl CH Fc), 71.4 (br., $C_{ipso}Si$), 69.5 (cyclopentadienyl CH fc), 68.8 (C_5H_5), 65.1 (cyclopentadienyl CH fc), 2.0 ppm ($SiMe_2$). $^{29}Si\{^1H\}$ NMR (C_6D_6): $\delta = -1.7$ ppm. ^{207}Pb NMR (C_6D_6): $\delta = 3913$ ppm.

Synthesis of [1Et(DMAP)]: A solution of **4Et** (74 mg, 0.19 mmol) and $[(Me_3Si)_2N]_2Pb$ (101 mg, 0.19 mmol) in toluene (2 mL) was heated to 70 °C for 1 h. DMAP (23 mg, 0.19 mmol) was added. The heating bath was removed and the solution allowed to cool to ambient temperature. Volatile components were removed under vacuum, leaving a yellow microcrystalline solid, which was recrystallized from *n*-hexane. Yield 126 mg (93%). $C_{25}H_{40}N_4FePbSi_2$ (715.85): C 41.95, H 5.63, N 7.83%; found: C 42.24, H 5.93, N 7.94%. ^1H NMR (C_6D_6): $\delta = 8.54$, 6.00 (2 br., 2×2 H, DMAP CH), 3.89, 3.83 (2 m, 2×4 H, fc), 2.08 (s, 6 H, NMe_2), 1.16 (t, $J_{HH} = 7.9$ Hz, 6 H, CH_2CH_3), 0.82 (q, $J_{HH} = 7.9$ Hz, 4 H, CH_2CH_3), 0.35 ppm (s, 12 H, $SiMe_2$). $^{13}C\{^1H\}$ NMR (C_6D_6): $\delta = 154.8$ ($CNMe_2$), 148.3 (DMAP CH), 117.0 (CNSi), 107.2 (DMAP CH), 69.1, 63.8 (2×cyclopentadienyl CH), 38.3 (NMe_2), 11.5 (CH_2), 8.4 (CH_2CH_3), 1.4 ppm ($SiMe_2$). $^{29}Si\{^1H\}$ NMR (C_6D_6): $\delta =$ 7.1 ppm. ^{207}Pb NMR (C_6D_6): $\delta = 3009$ ppm.

Synthesis of [1*i*Pr(DMAP)]: This compound was obtained as an orange crystalline solid by a procedure analogous to that described for **[1Et(DMAP)]** from **4*i*Pr** (230 mg, 0.55 mmol), $[(Me_3Si)_2N]_2Pb$ (292 mg, 0.55 mmol) and DMAP (67 mg, 0.55 mmol). Yield 340 mg (83%). $C_{27}H_{44}N_4FePbSi_2$ (743.90): C 43.59, H 5.96, N 7.53%; found: C 43.02, H 6.16, N 7.77%. ^1H NMR (C_6D_6): $\delta = 8.55$, 6.01 (2 br., 2×2 H, DMAP CH), 3.87, 3.82 (2 m, 2×4 H, fc), 2.09 (s, 6 H, NMe_2), 1.20 (m, 12 H, $CHMe_2$), 1.10 (m, 2 H, $CHMe_2$), 0.35 ppm (s, 12 H, $SiMe_2$). $^{13}C\{^1H\}$ NMR (C_6D_6): $\delta = 154.8$ ($CNMe_2$), 148.5 (DMAP CH), 117.1 (CNSi), 107.2 (DMAP CH), 68.9, 63.8 (2×cyclopentadienyl CH), 38.3 (NMe_2), 18.5 ($CHMe_2$), 16.8 ($CHMe_2$), −0.2 ppm ($SiMe_2$). $^{29}Si\{^1H\}$ NMR (C_6D_6): $\delta = 8.9$ ppm. ^{207}Pb NMR (C_6D_6): $\delta = 3023$ ppm.

Synthesis of [1Ph(DMAP)]: This compound was obtained as an orange crystalline solid by a procedure analogous to that described for **[1Et(DMAP)]** from **4Ph** (176 mg, 0.36 mmol), $[(Me_3Si)_2N]_2Pb$ (190 mg, 0.36 mmol) and DMAP (44 mg, 0.36 mmol). Yield 118 mg (40%). $C_{33}H_{40}N_4FePbSi_2$ (811.93): C 48.82, H 4.97, N 6.90%; found: C 47.92, H 4.93, N 6.66%. ^1H NMR (C_6D_6): $\delta = 8.37$ (m, 2 H, DMAP CH), 7.80, 7.30 (2 m, 2×4 H, Ph), 7.24 (m, 2 H, Ph), 5.92 (m, 2 H, DMAP CH), 3.91, 3.79 (2 m, 2×4 H, fc), 2.06 (s, 6 H, NMe_2), 0.58 ppm (s, 12 H, $SiMe_2$). $^{13}C\{^1H\}$ NMR (C_6D_6): $\delta = 154.8$ ($CNMe_2$), 148.4 (DMAP CH), 143.9 (Ph C_{ipso}), 134.5, 128.8, 127.9 (3×Ph CH), 116.3 (CNSi), 107.2 (DMAP CH), 69.0, 63.9 (2×cyclopentadienyl CH), 38.3 (NMe_2), 2.1 ppm ($SiMe_2$). $^{29}Si\{^1H\}$ NMR (C_6D_6): $\delta = -2.8$ ppm. ^{207}Pb NMR (C_6D_6): $\delta = 2928$ ppm.

Synthesis of [1Mes(DMAP)]: This compound was obtained as an orange crystalline solid by a procedure analogous to that described for **[1Et(DMAP)]** from **4Mes** (300 mg, 0.53 mmol), $[(Me_3Si)_2N]_2Pb$ (279 mg, 0.53 mmol) and DMAP (64 mg, 0.53 mmol). Benzene was used for recrystallization. Yield 373 mg (79%). $C_{39}H_{52}N_4FePbSi_2$ (896.09): C 52.27, H 5.85, N 6.25%; found: C 51.97, H 5.99, N 6.05%. ^1H NMR (C_6D_6): $\delta = 8.46$ (br., 2 H, DMAP CH), 6.74 (s, 4 H, $C_6H_2Me_3$), 6.02 (br., 2 H, DMAP CH), 3.91, 3.84 (2 m, 2×4 H, fc), 2.66 (s, 12 H, *o*-Me), 2.15 (s, 6 H, *p*-Me), 2.09 (s, 6 H, NMe_2), 0.69 ppm (s, 12 H, $SiMe_2$). $^{13}C\{^1H\}$ NMR (C_6D_6): $\delta = 154.7$ ($CNMe_2$), 148.4 (DMAP CH), 144.6, 138.4, 135.7 (3×C_{quat} Mes), 129.7 (CH Mes), 115.6 (CNSi), 107.2 (DMAP CH), 69.0, 63.9 (2×cyclopentadienyl CH), 38.3 (NMe_2), 25.7 (*o*-Me), 21.1 (*p*-Me), 8.2 ppm ($SiMe_2$). $^{29}Si\{^1H\}$ NMR (C_6D_6): $\delta =$ −4.3 ppm. ^{207}Pb NMR (C_6D_6): $\delta = 3121$ ppm.

Synthesis of [1Fc(DMAP)]: This compound was obtained as an orange crystalline solid by a procedure analogous to that described for **[1Et(DMAP)]** from **4Fc** (100 mg, 0.14 mmol), $[(Me_3Si)_2N]_2Pb$ (75 mg, 0.14 mmol) and DMAP (17 mg, 0.14 mmol). Toluene was used for recrystallization. Yield 123 mg (84%). $C_{41}H_{48}N_4Fe_3PbSi_2$ (1027.77): C 47.91, H 4.71, N 5.45%; found: C 46.46, H 4.75, N 5.07%. ^1H NMR (C_6D_6): $\delta = 8.48$, 6.06 (2 br., 2×2 H, DMAP CH), 4.21, 4.16 (2 m, 2×4 H, Fc), 4.03 (s, 10 H, C_5H_5), 3.92, 3.85 (2 m, 2×4 H, fc), 2.14 (s, 6 H, NMe_2), 0.59 ppm (s, 12 H, $SiMe_2$). $^{13}C\{^1H\}$ NMR (C_6D_6): $\delta =$ 154.5 ($CNMe_2$), 149.2 (DMAP CH), 117.0 (CNSi), 107.0 (DMAP CH), 75.2 ($C_{ipso}Si$), 74.0, 70.9 (2×cyclopentadienyl CH Fc), 69.2 (cyclopentadienyl CH fc), 68.7 (C_5H_5), 63.8 (cyclopentadienyl CH fc), 38.3 (NMe_2), 2.4 ppm ($SiMe_2$). $^{29}Si\{^1H\}$ NMR (C_6D_6): $\delta = -2.7$ ppm. ^{207}Pb NMR (C_6D_6): $\delta = 2991$ ppm.

X-ray crystallography: For each data collection a single crystal was mounted on a micro-mount and all geometric and intensity data were taken from this sample at 100(2) K. Data collections were carried out either on a Stoe IPDS2 diffractometer equipped with a 2-circle goniometer and an area detector on a Stoe StadiVari diffractometer equipped with a 4-circle goniometer and a DECTRIS Pilatus 200 K detector. The data sets were corrected for absorption, Lorentz and polarisation effects. The structures were solved by direct methods (SHELXT) and refined using alternating cycles of least-squares refinements against F^2 (SHELXL2014/7).[20] C-bonded H atoms were included in the models in calculated positions, heteroatom-bonded H atoms have been found in the difference Fourier lists. All H atoms were treated with the 1.2-fold or 1.5-fold

isotropic displacement parameter of their bonding partner. Experimental details for each diffraction experiment are given in Table S1 in the Supporting Information. CCDC 2249161–2249168 contain the supplementary crystallographic data for this paper. These data are provided free of charge by the joint Cambridge Crystallographic Data Centre and Fachinformationszentrum Karlsruhe Access Structures service.

Computational methods: All geometry optimizations and harmonic frequency calculations were performed using the ORCA program package (5.0.3).[21,22] For geometry optimisations the M06L[23] density functional combined with the def2-SVP[24] basis set was used. Zero-point vibrational energies and thermal contributions to Gibbs free energies at 298.15 K were obtained at this level of theory. To account for the overestimation of entropic contributions to Gibbs free energies we employ a standard-state conversion from 1 atm gas phase to 1 M solution. Additional single point calculations on optimised geometries were performed using the same functional and the def2-TZVPPD[24] basis set and the CPCM[25] implicit solvation model with benzene as the solvent. Optimised structures were characterised as minima or first-order saddle points by eigenvalue analysis of the computed Hessians. In the case of dimer **2Fc** (R = Fc) a low imaginary frequency remained even after displacement and reoptimisation corresponding to a slight tilting of a silicon-bonded Fc moiety. The resulting small uncertainty resulting to its free energy is, however, chemically irrelevant. Wave functions for bonding analyses on optimised geometries were obtained from single-point calculations in the Gaussian program package (Rev. B.01)[26] employing the M06-L density functional in combination with the 6-311 + + G(2d,2p)[27–32] basis set for H, C, N, Si, Fe and the cc-pVTZ-PP[33,34] basis set for Pb. QTAIM analyses were performed with the AIMALL program.[35]

Acknowledgements

Open Access funding enabled and organized by Projekt DEAL.

Conflict of Interests

The authors declare no conflict of interest.

Data Availability Statement

The data that support the findings of this study are available in the supplementary material of this article.

Keywords: carbene homologues · lead · metallocenes · steric hindrance · subvalent compounds

[1] a) C. D. Varnado Jr., E. L. Rosen, M. S. Collins, V. M. Lynch, C. W. Bielawski, *Dalton Trans.* **2013**, *42*, 13251–13264; b) E. L. Rosen, C. D. Varnado Jr., A. G. Tennyson, D. M. Khramov, J. W. Kamplain, D. H. Sung, P. T. Cresswell, V. M. Lynch, C. W. Bielawski, *Organometallics* **2009**, *28*, 6695–6706; c) D. M. Khramov, E. L. Rosen, V. M. Lynch, C. W. Bielawski, *Angew. Chem. Int. Ed.* **2008**, *47*, 2267–2270.
[2] Recent reviews: a) Y. Ryu, G. Ahumada, C. W. Bielawski, *Chem. Commun.* **2019**, *55*, 4451–4466; b) E. Peris, *Chem. Rev.* **2018**, *118*, 9988–10031.
[3] a) J. Zinke, C. Bruhn, U. Siemeling, *Z. Anorg. Allg. Chem.* **2023**, *649*, e202200334; b) B. A. Correia Bicho, R. Guthardt, C. Bruhn, D. Großhennig, T. Orth, F. Pfeiffer, U. Siemeling, *Eur. J. Inorg. Chem.* **2022**, e202101014; c) A. R. Petrov, A. Derheim, J. Oetzel, M. Leibold, C. Bruhn, S. Scheerer, S. Oßwald, R. F. Winter, U. Siemeling, *Inorg. Chem.* **2015**, *54*, 6657–6670; d) S. Rittinghaus, C. Färber, C. Bruhn, U. Siemeling, *Dalton Trans.* **2014**, *43*, 3508–3520; e) U. Siemeling, C. Färber, M. Leibold, C. Bruhn, P. Mücke, R. F. Winter, B. Sarkar, M. von Hopffgarten, G. Frenking, *Eur. J. Inorg. Chem.* **2009**, 4607–4612; f) U. Siemeling, C. Färber, C. Bruhn, *Chem. Commun.* **2009**, 98–100.
[4] a) C. Goedecke, M. Leibold, U. Siemeling, G. Frenking, *J. Am. Chem. Soc.* **2011**, *133*, 3557–3569; b) U. Siemeling, C. Färber, C. Bruhn, M. Leibold, D. Selent, W. Baumann, M. von Hopffgarten, C. Goedecke, G. Frenking, *Chem. Sci.* **2010**, *1*, 697–704.
[5] For selected reviews, see: a) H. Kim, E. Lee, *Bull. Korean Chem. Soc.* **2022**, *43*, 1328–1341; b) I. Alkorta, J. Elguero, *J. Heterocycl. Chem.* **2019**, *56*, 359–370; c) H. Song, Y. Kim, J. Park, K. Kim, E. Lee, *Synlett* **2016**, *27*, 477–485; d) S. Yadav, S. Saha, S. S. Sen, *ChemCatChem* **2016**, *8*, 486–501; e) U. Siemeling, *Aust. J. Chem.* **2011**, *64*, 1109–1112; f) D. Martin, M. Soleilhavoup, G. Bertrand, *Chem. Sci.* **2011**, *2*, 389–399.
[6] a) N. Weyer, M. Heinz, C. Bruhn, M. C. Holthausen, U. Siemeling, *Chem. Commun.* **2021**, *57*, 9378–9381; b) N. Weyer, M. Heinz, J. I. Schweizer, C. Bruhn, M. C. Holthausen, U. Siemeling, *Angew. Chem. Int. Ed.* **2021**, *60*, 2624–2628; c) R. Guthardt, C. Bruhn, U. Siemeling, *Polyhedron* **2021**, *194*, 114959; d) R. Guthardt, C. Bruhn, C. Färber, U. Siemeling, *Organometallics* **2020**, *39*, 4174–4177; e) R. Guthardt, D. Bachmann, C. Bruhn, U. Siemeling, *Z. Anorg. Allg. Chem.* **2020**, *646*, 761–768; f) R. Guthardt, J. Oetzel, J. I. Schweizer, C. Bruhn, R. Langer, M. Maurer, J. Vícha, P. Shestakova, M. C. Holthausen, U. Siemeling, *Angew. Chem. Int. Ed.* **2019**, *58*, 1387–1391; g) N. Weyer, R. Guthardt, B. A. Correia Bicho, J. Oetzel, C. Bruhn, U. Siemeling, *Z. Anorg. Allg. Chem.* **2019**, *645*, 188–197; h) J. Oetzel, C. Bruhn, U. Siemeling, *Z. Anorg. Allg. Chem.* **2018**, *644*, 935–944; i) J. Volk, B. A. Correia Bicho, C. Bruhn, U. Siemeling, *Z. Naturforsch. B* **2017**, *72*, 785–794; j) J. Oetzel, N. Weyer, C. Bruhn, M. Leibold, B. Gerke, R. Pöttgen, M. Maier, R. F. Winter, M. C. Holthausen, U. Siemeling, *Chem. Eur. J.* **2017**, *23*, 1187–1199; see also: k) F. Walz, E. Moos, D. Garnier, R. Köppe, C. E. Anson, F. Breher, *Chem. Eur. J.* **2017**, *23*, 1173–1186.
[7] R. Guthardt, J. Blanckenberg, C. Bruhn, U. Siemeling, *Chem. Commun.* **2021**, *57*, 12984–12987.
[8] **4Et**, **4*i*Pr**, **4Mes**, and **4Fc** are new compounds, which were obtained in analogy to known homologues (see the Experimental Section). The latter two have been structurally characterised by XRD (see the Supporting Information).
[9] The unusual chemical shift may be ascribed to the deshielding heavy-atom effect of lead, which induces a spin-orbit contribution to the light-atom chemical shift; see: a) J. Vícha, J. Novotný, S. Komorovsky, M. Straka, M. Kaupp, R. Marek, *Chem. Rev.* **2020**, *120*, 7065–7103; b) J. Autschbach, in: *High Resolution NMR Spectroscopy – Understanding Molecules and Their Electronic Structures* (Ed.: R. H. Contreras), Elsevier, Amsterdam, **2013**, pp. 69–117.
[10] Seminal paper: S. Winstein, N. J. Holness, *J. Am. Chem. Soc.* **1955**, *77*, 5562–5578.
[11] Values (rounded to the first decimal) taken from: E. L. Eliel, S. H. Wilen, *Organische Stereochemie*, Wiley-VCH, Weinheim, **1998**, pp. 443–444.
[12] B. Wrackmeyer, *Annu. Rep. NMR Spectrosc.* **2002**, *47*, 1–37.
[13] B. Wrackmeyer, K. Horchler, H. Zhou, *Spectrochim. Acta Part A* **1990**, *46*, 809–816.
[14] G. G. Briand, A. D. Smith, G. Schatte, A. J. Rossini, R. W. Schurko, *Inorg. Chem.* **2007**, *46*, 8625–8637.
[15] M. J. S. Gynane, D. H. Harris, M. F. Lappert, P. P. Power, P. Rivière, M. Rivière-Baudet, *J. Chem. Soc. Dalton Trans.* **1977**, 2004–2009.
[16] C. Thie, C. Bruhn, U. Siemeling, *Eur. J. Inorg. Chem.* **2015**, 5457–5466.
[17] S.-O. Hauber, M. Niemeyer, *Z. Anorg. Allg. Chem.* **2008**, *634*, 2594–2600.
[18] M. Herberhold, A. Ayazi, W. Milius, B. Wrackmeyer, *J. Organomet. Chem.* **2002**, *656*, 71–80.
[19] S. Duhović, P. L. Diaconescu, *Polyhedron* **2013**, *52*, 377–388.
[20] G. M. Sheldrick, *Acta Crystallogr. Sect. A* **2008**, *64*, 112–122.
[21] F. Neese, *Wiley Interdiscip. Rev.: Comput. Mol. Sci.* **2012**, *2*, 73–78.
[22] F. Neese, *WIREs Comput. Mol. Sci.* **2022**, *12*, e1606.
[23] Y. Zhao, D. G. Truhlar, *J. Chem. Phys.* **2006**, *125*, 194101.
[24] F. Weigend, R. Ahlrichs, *Phys. Chem. Chem. Phys.* **2005**, *7*, 3297–3305.
[25] V. Barone, M. Cossi, *J. Phys. Chem. A* **1998**, *102*, 1995–2001.
[26] M. J. Frisch, G. W. Trucks, H. B. Schlegel, G. E. Scuseria, M. A. Robb, J. R. Cheeseman, G. Scalmani, V. Barone, G. A. Petersson, H. Nakatsuji, X. Li, M. Caricato, A. V. Marenich, J. Bloino, B. G. Janesko, R. Gomperts, B. Mennucci, H. P. Hratchian, J. V. Ortiz, A. F. Izmaylov, J. L. Sonnenberg, D. Williams-Young, F. Ding, F. Lipparini, F. Egidi, J. Goings, B. Peng, A. Petrone, T. Henderson, D. Ranasinghe, V. G. Zakrzewski, J. Gao, N. Rega,

G. Zheng, W. Liang, M. Hada, M. Ehara, K. Toyota, R. Fukuda, J. Hasegawa, M. Ishida, T. Nakajima, Y. Honda, O. Kitao, H. Nakai, T. Vreven, K. Throssell, J. A. Montgomery Jr., J. E. Peralta, F. Ogliaro, M. J. Bearpark, J. J. Heyd, E. N. Brothers, K. N. Kudin, V. N. Staroverov, T. A. Keith, R. Kobayashi, J. Normand, K. Raghavachari, A. P. Rendell, J. C. Burant, S. S. Iyengar, J. Tomasi, M. Cossi, J. M. Millam, M. Klene, C. Adamo, R. Cammi, J. W. Ochterski, R. L. Martin, K. Morokuma, O. Farkas, J. B. Foresman, D. J. Fox, Wallingford, CT, **2016**.
[27] A. D. McLean, G. S. Chandler, *J. Chem. Phys.* **1980**, *72*, 5639–5648.
[28] R. Krishnan, J. S. Binkley, R. Seeger, J. A. Pople, *J. Chem. Phys.* **1980**, *72*, 650–654.
[29] T. Clark, J. Chandrasekhar, G. W. Spitznagel, P. V. R. Schleyer, *J. Comput. Chem.* **1983**, *4*, 294–301.
[30] M. J. Frisch, J. A. Pople, J. S. Binkley, *J. Chem. Phys.* **1984**, *80*, 3265–3269.
[31] P. J. Hay, *J. Chem. Phys.* **1977**, *66*, 4377–4384.
[32] A. J. H. Wachters, *J. Chem. Phys.* **1970**, *52*, 1033–1036.
[33] K. A. Peterson, *J. Chem. Phys.* **2003**, *119*, 11099–11112.
[34] B. Metz, H. Stoll, M. Dolg, *J. Chem. Phys.* **2000**, *113*, 2563–2569.
[35] T. A. Keith, *AIMALL (Version 17.01.25)* **2016**, Overlad Park KS, USA, http://aim.tkgristmill.com.

Manuscript received: March 28, 2023
Revised manuscript received: May 8, 2023
Accepted manuscript online: May 12, 2023
Version of record online: May 17, 2023